

- 2 CARROLL, J.M., and CHANG, K.: 'Microstrip mode suppression ring resonator', *Electron. Lett.*, 1994, **30**, pp. 1861-1862
- 3 MARTI, J., and GRIOL, A.: 'Harmonic suppressed microstrip multistage coupled ring bandpass filters', *Electron. Lett.*, 1998, **34**, pp. 2140-2142
- 4 TRABELSI, H., CRUCHON, C., and ALQUIE, G.: 'Microwave frequency agile active filter with distributed and MMIC elements', *Electron. Lett.*, 1998, **34**, pp. 2135-2136
- 5 KARACA OGLU, U., ROBERTSON, I.D., and GUGLIELMI, M.: 'A dual-mode microstrip ring resonator filter with active devices for loss compensation'. IEEE Int. Microwave Symp. Dig., 1993, pp. 189-192
- 6 WOLFF, I., and KNOPPIK, N.: 'Microstrip ring resonator and dispersion measurement on microstrip lines', *Electron. Lett.*, 1971, **7**, pp. 779-781

## Hough transform network

J. Basak and S.K. Pal

A two-layered Hough transform network is proposed which accepts image co-ordinates as the input and learns the parametric forms of the lines in the image adaptively. It provides an efficient representation of visual information embedded in the connection weights. It not only reduces the large space requirements, as in the case of the classical Hough transform, but also represents the parameters with high precision.

**Introduction:** The Hough transform [1] is a transformation from image space to parameter space in such a way that pixels belonging to a straight line form a cluster in the parameter space. A straight line can be parametrically expressed as

$$r = x_1 \cos \phi + x_2 \sin \phi \quad (1)$$

where  $(x_1, x_2)$  is the co-ordinate of any point on the straight line and  $(r, \phi)$  are the parameters of the straight line. Any point on the straight line in the image space can be viewed as a curve (sinusoidal in nature) in the parameter space passing through the point  $(r, \phi)$ . The parameter space is quantised and each slot represents a range  $(\Delta r, \Delta \phi)$ . An accumulator array  $(A)$  is defined such that for any  $(r_0, \phi_0)$ ,  $A(r_0, \phi_0)$  is incremented by unity if any parameter value in the range  $(r_0 \pm \Delta r/2, \phi_0 \pm \Delta \phi/2)$  satisfies eqn. 1 corresponding to a pixel. Thus from the effect of all pixels on the straight line in the image space, a local peak in the accumulator values will be formed around  $(r, \phi)$ . The straight line in the image can then be identified by detecting the local peaks in the accumulator. This technique has natural extensions for detecting curves and arbitrary shapes [2]. The identification of peaks in the quantised parameter (accumulator) space is one of the major problems behind applying the Hough transform to real life problems. It is often difficult to obtain the peaks by thresholding since the selection of the threshold is very much subjective and an improper selection may lead to several spurious peaks. Moreover, space requirements are another major problem of the Hough transform. For higher precision, if the slots are chosen to be very small then the required storage space becomes enormous. Also, this leads to the peak response being distributed over the neighbouring slots. On the other hand, for coarse quantisation, the precision in estimating the parameters becomes reduced.

Here we describe a two layer neural network model, namely, the Hough transform network, for calculating the Hough transform. The network consists of two layers: input and output. Each output node is connected to all input nodes. The number of input nodes is equal to the dimensionality of the input space. For example, the network consists of only two input nodes when it accepts the image co-ordinates (in the object region) as the input. The number of output nodes is chosen to be equal to the number of straight line segments in the image. The connection weights from the input layer to any particular output node along with the threshold of the output node represent the parameter values of the corresponding straight line segment (or the hyperplane in the case of a higher dimensional input). The network accepts the image co-ordinates (i.e.,  $(x_1, x_2)$ ) as in eqn. 1) sequentially as the input and learns adaptively the parameter values in the form of connection weights in an unsupervised mode. The activation in the output layer indi-

cates the straight line segment(s) (or hyperplane) to which the input pixel (or input vector) belongs.

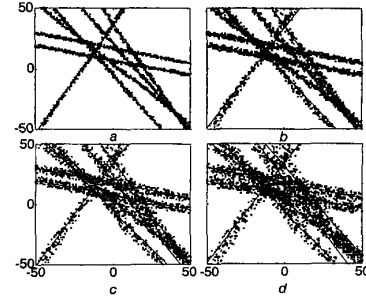


**Fig. 1** Straight lines extracted by Hough transform network  
Maximum shifts in pixel locations: a 1, b 2, c 3, d 5

**Learning Hough transform:** Eqn. 1 can be represented as

$$\sum w_i x_i = \theta \quad (2)$$

where  $\mathbf{x} = (x_1, x_2)$  is the co-ordinate of a pixel in the object region of the image. In the case of a higher dimensional input,  $\mathbf{x} = (x_1, x_2, \dots, x_n)$  represents a variable on the hyperplane to be identified.  $\theta$  is the distance of the straight line (hyperplane in the case of a higher dimension) from the origin (in the Euclidian sense), i.e.  $\theta = r$ , and  $\sum w_i^2 = 1$ . A set of  $m$  such straight lines (or hyperplanes) can be represented as  $\mathbf{W}\mathbf{x} = \theta$ , where  $\mathbf{W}$  is an  $m \times n$ , matrix and  $\theta$  is an  $m \times 1$  vector. Each row of  $\mathbf{W}$  corresponds to the parameter set of one hyperplane, i.e.  $\sum_j w_{ij}^2 = 1$  for all  $i$ .

Corresponding to  $\mathbf{x}$ , the input to the neural network, the output  $\mathbf{y}$  is given as

$$\mathbf{y} = \mathbf{f}(\mathbf{u}) = [f(u_1), f(u_2), \dots, f(u_m)] \quad (3)$$

where  $\mathbf{u}$  is the input to the output neurons, given as

$$\mathbf{u} = \mathbf{W}\mathbf{x} - \theta \quad (4)$$

$f(\cdot)$  is a bell-shaped transfer function with peak at zero. We have chosen a Gaussian form of the function, i.e.

$$y_i = \exp(-u_i^2 / \lambda^2) \quad (5)$$

If  $\mathbf{x}$  belongs to the  $i$ th hyperplane then  $u_i = 0$ , i.e.  $y_i = 1$ , otherwise  $y_i < 1$ . To learn  $\mathbf{W}$  and  $\theta$ , an objective function (a continuous and differentiable one)

$$E = \left[ \prod_{i=1}^n (1 - y_i) \right]^\alpha \quad (6)$$

is chosen such that it is zero when  $y_i$  is zero for any  $i$ . The parameter  $\alpha > 0$  determines the steepness of the function near minima (i.e. a fixed point). As  $\alpha$  increases, the steepness decreases. The weight matrix  $\mathbf{W}$  and  $\theta$  are updated in order to decrease  $E$ . Following the steepest gradient descent rule, the weight updating is given as

$$\Delta w_{ij} = -\beta \frac{\partial E}{\partial w_{ij}} = \frac{\gamma E}{1 - y_i} f'(u_i) x_j \quad (7)$$

where  $\beta$  is a constant of proportionality and  $\gamma = \alpha\beta$ . Similarly, the change in  $\theta$  can be represented as

$$\Delta \theta_i = -[k\gamma E / (1 - y_i)] f'(u_i) \quad (8)$$

The learning rate for  $\theta$  is considered to be  $k\gamma$ , where  $k$  is a constant. The change in  $w_{ij}$  should be such that at any iteration  $\sum_j w_{ij}^2(t) = 1$  for all  $i$ . After normalisation of  $\mathbf{W}$ , the updating rule is

$$w_{ij}(t+1) = \frac{w_{ij}(t) + \Delta w_{ij}(t)}{\left[ \sum_j (w_{ij}(t) + \Delta w_{ij}(t))^2 \right]^{1/2}} \quad (9)$$

Considering  $\sum_j w_{ij}^2(t) = 1$ , and  $\Delta w_{ij}(t)$  to be sufficiently small with respect to  $w_{ij}(t)$ ,

$$w_{ij}(t+1) =$$

$$w_{ij}(t) + \frac{\gamma E}{1 - y_i(t)} f'(u_i(t)) (x_j(t) - w_{ij}(t)(u_i(t) + \theta_i(t))) \quad (10)$$

Note that, in the principal component analysis network [3] also, the same kind of normalisation is performed with different activation functions. From eqns. 5 and 10, the learning rule becomes

$$\begin{aligned} w_{ij}(t+1) &= w_{ij}(t) - \frac{2\gamma E}{\lambda^2} \left( \frac{y_i(t)}{1 - y_i(t)} \right) u_i(t) [x_j(t) \\ &\quad - w_{ij}(t)(u_i(t) + \theta_i(t))] \\ \theta_i(t+1) &= \theta_i(t) + \frac{2k\gamma E}{\lambda^2} \left( \frac{y_i(t)}{1 - y_i(t)} \right) u_i(t) \end{aligned} \quad (11)$$

The parameter  $\lambda$  determines the width of the bell shaped activation function. For small values of  $\lambda$ , the activation function is highly localised. Therefore the hyperplanes become slightly perturbed by the distant points. This is necessary when the dynamics of the network settles to the desired stable state. On the other hand, for large  $\lambda$  the attraction of the hyperplanes towards the distant points are small, thereby, making the network very inefficient.

Let, in the vicinity of the desired fixed point, the weight matrix  $\mathbf{W}$  and  $\theta$  be perturbed in such a way that it makes the objective function  $E$  zero for the given sample point, i.e.

$$E(t+1) = E(t) \left[ \prod_i \left( 1 - \frac{\Delta y_i}{1 - y_i} \right) \right]^\alpha = 0 \quad (12)$$

where  $\Delta \mathbf{y} = [\Delta y_1, \Delta y_2, \dots, \Delta y_n]$  is the change in output due to the updating of  $\mathbf{W}$  and  $\theta$ . Near the fixed point (minima), the required change in  $\mathbf{y}$  is small and therefore we can restore only the first order terms of  $\Delta \mathbf{y}$  in eqn. 12, i.e.

$$E(t) \left( 1 - \alpha \sum_i \frac{\Delta y_i}{1 - y_i} \right) = 0$$

Therefore

$$\sum_i \frac{\Delta y_i}{1 - y_i} = \frac{1}{\alpha} \quad (13)$$

The change in  $\mathbf{u}$  is given as

$$\begin{aligned} \Delta u_i(t) &= u_i(t+1) - u_i(t) \\ &= -\frac{2\gamma E}{\lambda^2} \left( \frac{y_i}{1 - y_i} \right) u_i [k + X - (u_i + \theta_i)^2] \end{aligned} \quad (14)$$

where  $\mathbf{X} = \sum_j x_j^2$ . The change in the output  $\mathbf{y}$  for small changes in  $\mathbf{u}$  can be written as

$$\Delta y_i = -(2u_i/\lambda^2) y_i \Delta u_i \quad (15)$$

From eqns. 13 – 15, we obtain

$$\frac{4\gamma E}{\lambda^2} \sum_i \left( \frac{y_i}{1 - y_i} \right)^2 \log \left( \frac{1}{y_i} \right) [k + X - (u_i + \theta_i)^2] = \frac{1}{\alpha} \quad (16)$$

Therefore, the learning rules for  $\mathbf{W}$  and  $\theta$  are

$$\begin{aligned} \Delta w_{ij}(t) &= \\ &= \frac{u_i(t) \left( \frac{y_i(t)}{1 - y_i(t)} \right) [x_j(t) - w_{ij}(t)(u_i(t) + \theta_i(t))]}{2\alpha \sum_k \left( \frac{y_k(t)}{1 - y_k(t)} \right)^2 \log \left( \frac{1}{y_k(t)} \right) [k + X - (u_k(t) + \theta_k(t))^2]} \end{aligned} \quad (17)$$

$$\Delta \theta_i(t) = \frac{u_i(t) \left( \frac{y_i(t)}{1 - y_i(t)} \right)}{2\alpha \sum_k \left( \frac{y_k(t)}{1 - y_k(t)} \right)^2 \log \left( \frac{1}{y_k(t)} \right) [k + X - (u_k(t) + \theta_k(t))^2]} \quad (18)$$

The updating rules reveal the fact that the changes in the parameter values are independent of the selection of  $\lambda$ . The parameter  $\lambda$ , however, is implicitly embedded in the output  $\mathbf{y}$  of the network. Initially, when the parameter values of the network are far from the fixed point, the denominator is very small. To account for this situation, the learning rate is clamped to a constant value when

the denominator is very small. Near the optimal solution, the learning rate changes according to eqns. 17 and 18.

Seven different straight lines are synthetically generated in a 100 × 100 image. The pixels on the straight lines are randomly shifted both horizontally and vertically. The maximum shifts in pixel locations are 1, 2, 3, and 5 as shown in Fig. 1a–d, respectively. Parameters  $\alpha$  and  $\lambda$  are chosen as 2 and 5, respectively. The learning rate is clamped to 0.05/ $\alpha$  when the denominators of eqns. 17 and 18 are less than 20 $\alpha$ . The value of  $k$  is taken to be equal to the average distance of the points from the origin. The straight lines depicted are those identified by the network.

**Conclusions:** The Hough transform network is able to learn the parametric forms of the lines in all unsupervised manner, and provides an efficient model for the learning and representation of visual information. The space requirements are much lower than those of the classical Hough transform and also the parameters can be represented with very high precision. The network can be naturally generalised to higher order models for determining curves and arbitrary shapes. Here the number of line segments present in the image is assumed to be known. This restriction can also be relaxed by incorporating the self-organising mechanisms into the network.

© IEE 1999

11 February 1999

Electronics Letters Online No: 19990283  
DOI: 10.1049/el:19990283

J. Basak and S.K. Pal (Machine Intelligence Unit, Indian Statistical Institute, Calcutta 700 035, India)

## References

- 1 BALLARD, D., and BROWN, C.: 'Computer vision' (Prentice-Hall Inc., Englewood Cliffs, NJ, 1982)
- 2 BALLARD, D.H.: 'Generalizing the Hough transform to detect arbitrary shapes', *Pattern Recogn.*, 1981, **13**, pp. 111–122
- 3 OJA, E., KARHUNEN, J., WANG, L., and VIGANO, R.: 'Principal and independent components in neural networks - recent developments'. Proc. Italian Workshop on Neural Networks, WIRN'95, Vietri, Italy, 1995

## 2.5Gbit/s free space optical link over 4.4km

G. Nykolak, P.F. Szajowski, G. Tourgee and H. Presby

A new record in terrestrial free space optical transmission, 2.5Gbit/s (single channel) over a 4.4km range is reported. Optical data are transmitted over a horizontal path through the atmosphere, error free, using a specially designed optical telescope-transceiver, a conventional 1550nm laser transmitter, 2.5Gbit/s receiver/regenerator and a high power optical amplifier.

**Introduction:** Terrestrial free space optical communications is becoming an attractive alternative or adjunct to both RF wireless and, in some instances, to fibre as well. Free space optical communication is licence free, and secure over a line-of-site link. By combining advances in device technology taken from 1550nm fibre optical systems with new telescope designs, free space optical communications can provide multi-gigabit transmission capacities in a cost effective manner with high availability [1].

Our demonstration uses a pair of custom developed optical telescope terminals, a directly modulated DFB 1550nm laser and a 2.5Gbit/s digital lightwave receiver/regenerator. The input to the free space optical terminal is a singlemode fibre. The optical signal from a directly modulated DFB laser source is connected to the terminal's input. This signal is equally divided three ways and sent to three separate transmitting apertures, that are part of the terminal unit. Each aperture element is adjusted to provide approximately 0.5mrad divergence to the existing beam. In this way, the transmission path through the optical terminal is completely optically transparent. The receiver portion of the optical terminal uses a Schmidt-Cassegrain telescope configuration, with an effective receiving area of 0.025m<sup>2</sup>. The transmitted free space optical signal enters the receiving terminal and is effectively coupled to a